DNA Synthesis Generates Terminal Duplications That Seal End-to-End Chromosome Fusions

Mia Rochelle Lowden, *et al.*

Science **332**, 468 (2011);
DOI: 10.1126/science.1199022

is recovered in *slk19*Δ and *cdc14* mutant cells when replacing Sli15 with its constitutively dephosphorylated form, Sli15-6A (*13*). Expression of *SLI15-6A* in *slk19*Δ cells restored chromosome compaction and segregation to near wild-type levels. Thus, Ipl1 must be on the midzone to adapt condensation of endogenous long chromosomes (Fig. 4, A and B). Because *SLI15-6A* did not rescue the localization of separase in *slk19*Δ cells (fig. S9), Ipl1 regulated condensation independently of separase localization.

To examine the effects of midzone-bound Ipl1 on the segregation of long chromosomes, we visualized the distal region of *LC(XII:IV)cen4*Δ, marked by the *TRP1* locus (2.8 Mb from *CEN12*), in *slk19*Δ mutants. Separation of the distal *TRP1* locus, but not of a centromere-proximal one, was delayed in *slk19*Δ mutants ($P < 0.001$) (Fig. 4, B to D). As a consequence of this delay, spindle breakdown preceded *TRP1* segregation in 27% of *LC(XII:IV)cen4*Δ *slk19*Δ mutant cells (Fig. 4, C and E). Expression of *SLI15-6A* largely suppressed these defects (Fig. 4E). Thus, Slk19 affected segregation mainly through targeting of Ipl1/Aurora-B to the spindle midzone, which was especially important for the segregation of long chromosomes.

Together, our results indicate that yeast cells adjust the compaction of chromosomes to secure their segregation by the spindle. One key component of the underlying "ruler" may be the anaphase spindle, acting through the kinase aurora B at the midzone. Because long chromosome arms are exposed longer to the midzone than short ones, this model (fig. S11) accounts for their increased compaction and explains why compaction is also greater in the daughter cell. This simple model could also explain how small cells, with short spindles, still segregate their chromosomes at mitosis. Indeed, small cells such as *whi3*Δ mutants (*16*) hypercondensed their native chromosome IV (fig. S12), indicating that natural chromosomes adapt their compaction to anaphase spindle length.

Large variations in cell size and spindle length are common within species, and hyperlong chromosomes are well tolerated, at least in *Drosophila* (*17*). Similarly, chromosome rearrangements can increase chromosome size without diminishing cellular proliferation during cancer (*18*) or during size variations of rDNA loci (*19*). Perhaps spindle length and the level of chromosome condensation are not predetermined but are mutually coordinated through feedback regulatory loops. The mechanism described here is likely to be only one of such coupling systems. These probably play important roles not only during cell size changes but also in allowing chromosome rearrangements during speciation (*20*) and the survival of chromosomally unstable cancers (*21*).

References and Notes

1. D. C. Bouck, A. P. Joglekar, K. S. Bloom, *Annu. Rev. Genet.* **42**, 335 (2008).
2. A. J. Holland, D. W. Cleveland, *Nat. Rev. Mol. Cell Biol.* **10**, 478 (2009).
3. Materials and methods are available as supporting material on *Science* Online.
4. A. Hill, K. Bloom, *Mol. Cell. Biol.* **7**, 2397 (1987).
5. A. C. Vas, C. A. Andrews, K. Kirkland Matesky, D. J. Clarke, *Mol. Biol. Cell* **18**, 557 (2007).
6. B. D. Harrison, M. L. Hoang, K. Bloom, *Chromosoma* **118**, 633 (2009).
7. S. Buvelot, S. Y. Tatsutani, D. Vermaak, S. Biggins, *J. Cell Biol.* **160**, 329 (2003).
8. F. Mora-Bermúdez, D. Gerlich, J. Ellenberg, *Nat. Cell Biol.* **9**, 822 (2007).
9. B. D. Lavoie, E. Hogan, D. Koshland, *Genes Dev.* **18**, 76 (2004).
10. T. U. Tanaka *et al.*, *Cell* **108**, 317 (2002).
11. S. J. Nowak, V. G. Corces, *Trends Genet.* **20**, 214 (2004).
12. F. Stegmeier, R. Visintin, A. Amon, *Cell* **108**, 207 (2002).
13. G. Pereira, E. Schiebel, *Science* **302**, 2120 (2003).
14. M. Sullivan, F. Uhlmann, *Nat. Cell Biol.* **5**, 249 (2003).
15. A. Khmelinskii, C. Lawrence, J. Roostalu, E. Schiebel, *J. Cell Biol.* **177**, 981 (2007).
16. R. S. Nash, T. Volpe, B. Futcher, *Genetics* **157**, 1469 (2001).
17. W. Sullivan, D. R. Daily, P. Fogarty, K. J. Yook, S. Pimpinelli, *Mol. Biol. Cell* **4**, 885 (1993).
18. F. Mitelman, B. Johansson, F. Mertens, *Nat. Rev. Cancer* **7**, 233 (2007).
19. T. Kobayashi, D. J. Heck, M. Nomura, T. Horiuchi, *Genes Dev.* **12**, 3821 (1998).
20. A. Coghlan, E. E. Eichler, S. G. Oliver, A. H. Paterson, L. Stein, *Trends Genet.* **21**, 673 (2005).
21. H. Rajagopalan, C. Lengauer, *Nature* **432**, 338 (2004).

Acknowledgments: We thank P. Meraldi, Z. Shcheprova, C. Weirich, and S. Buvelot for helpful comments and critical reading of the manuscript; D. Clarke (University of Minnesota) for reagents; C. Iannone and R. Tejedor for help with qPCR; F. Campelo for help with statistical analysis; the ETH Light Microscopy Center; the CRG Advanced Light Microscopy Unit; and the CRG Ultrasequencing Unit. This project was supported by grants from La Caixa to G.N., the Spanish Ministry of Science to T.G. (BFU09-09168) and M.M. (BFU09-08213), and the Swiss National Science Foundation to Y.B.

Supporting Online Material

www.sciencemag.org/cgi/content/full/science.1201578/DC1
Materials and Methods
SOM Text
Figs. S1 to S12
Table S1
References

13 December 2010; accepted 28 February 2011
Published online 10 March 2011;
10.1126/science.1201578

DNA Synthesis Generates Terminal Duplications That Seal End-to-End Chromosome Fusions

Mia Rochelle Lowden,[1,2] Stephane Flibotte,[3] Donald G. Moerman,[3] Shawn Ahmed[1,2]*

End-to-end chromosome fusions that occur in the context of telomerase deficiency can trigger genomic duplications. For more than 70 years, these duplications have been attributed solely to breakage-fusion-bridge cycles. To test this hypothesis, we examined end-to-end fusions isolated from *Caenorhabditis elegans* telomere replication mutants. Genome-level rearrangements revealed fused chromosome ends having interrupted terminal duplications accompanied by template-switching events. These features are very similar to disease-associated duplications of interstitial segments of the human genome. A model termed Fork Stalling and Template Switching has been proposed previously to explain such duplications, where promiscuous replication of large, noncontiguous segments of the genome occurs. Thus, a DNA synthesis–based process may create duplications that seal end-to-end fusions, in the absence of breakage-fusion-bridge cycles.

Most human somatic cells are deficient for telomerase and experience progressive loss of telomeric DNA at chromosome ends. Critically shortened telomeres can elicit high levels of end-to-end chromosome fusion, resulting in genome rearrangements that commonly occur in developing tumors (*1*). In many organisms, the instability of dicentric chromosomes impedes elucidation of the initial structures of fusions events and, therefore, a mechanistic understanding of their genesis (Fig. 1A). Because *Caenorhabditis elegans* has holocentric chromosomes, end-to-end fusions derived from telomerase-deficient backgrounds can be transmitted stably during mitosis and meiosis (Fig. 1A). In other organisms, subtelomeric duplications that occur at critically shortened telomeres have been attributed to chromosome fusion followed by breakage during mitosis: the breakage-fusion-bridge (BFB) model (*2*, *3*). To test the hypothesis, we genetically isolated *C. elegans* end-to-end chromosome fusions on the basis of the meiotic nondisjunction phenotype that they cause when heterozygous (*4*–*6*).

[1]Department of Genetics, University of North Carolina, Chapel Hill, NC 27599, USA. [2]Department of Biology, University of North Carolina, Chapel Hill, NC 27514, USA. [3]Department of Zoology, University of British Columbia, Vancouver, British Columbia V6T 1Z4, Canada.

*To whom correspondence should be addressed. E-mail: shawn@med.unc.edu

These fusions were isolated from mutants deficient for the *trt-1* telomerase reverse transcriptase or for the DNA damage checkpoint gene *mrt-2*, which is required for telomerase-mediated telomere repeat addition (*4*, *5*). Homozygous fusions were then stably maintained, as assessed by genetic mapping and chromosome cytology, in strains having normal telomerase activity (*7*).

The molecular structures of 38 *X*-autosome end-to-end chromosome fusion events derived from *C. elegans trt-1* mutant strains were investigated using a whole-genome oligonucleotide microarray by comparative genomic hybridization (CGH) (*8*, *9*). Subtelomeric duplications were present at one (n = 17), both (n = 12), or neither (n = 9) of the fused chromosome ends (figs. S1 and S2). Duplicated regions ranged in size from 100 base pairs (bp) to 2.1 Mb and were typically two, three, or four times wild-type copy number (tables S1 and S2). Subtelomeric deletions frequently occurred before duplication (*7*), presumably as a consequence of end-resection of critically shortened telomeres.

In the BFB model, breakage of a sister chromatid fusion during anaphase may yield daughter cells with broken chromosomes carrying either a terminal deletion or an inverted duplication (Fig. 1A) (*10*). BFB-type inverted duplications could occur in *C. elegans* if holocentric sister chromatids fuse in G_2 and are then pulled toward opposite sides of the mitotic spindle and severed (Fig. 1A and fig. S3). CGH and/or sequencing revealed uninterrupted duplications consistent with BFB for 18 out of 41 fused chromosome termini (Fig. 2B and figs. S5B and S7). For example, the fusion *ypT43* (*X*R-*II*R) (chromosome number in italics; R, right end) is sealed by a 15.4-kb uninterrupted duplication of *II*R that is inverted with respect to the parent chromosome *II* (fig. S5B), which suggests sister chromatid fusion of *II*R and breakage, before fusion with *X*. The remaining 23 out of 41 fused chromosome termini had structures that ruled out BFB: regions present at two times wild-type copy number were typically punctuated by deletions or segments present at one, three, or four times wild-type copy number (Figs. 1, B and C; 2, B to D; and 3).

To characterize some of the chromosome rearrangements in detail, we used polymerase chain reaction (PCR) analysis to amplify fusion junctions and thereby to reveal the orientation and connectivity of the chromosome segments. An inverse PCR (iPCR) approach used primers targeted to a single chromosome end, which revealed recombination or end-joining with interstitial sites in the genome for complex fusions *ypT21*, *ypT27*, *ypT29*, *ypT50*, and *eT6* (n = 26 tested) [fig. S4 and supporting online material (SOM) Text]. The fusion junctions coincided with borders of genomic duplications observed by CGH (Fig. 2, B to D, and figs. S5A and S7; iPCR in blue font on CGH plots). A second PCR approach used robust, validated primers at borders of copy number changes to span rearrangement junctions predicted on the basis of CGH data alone. Eighteen sequence transitions were recovered for nine fusions (*ypT27*, *ypT29*, *ypT50*, *ypT23*, *ypT46*, *ypT49*, *ypT43*, *ypT35*, and *ypT37*; n = 12 tested) (table S3). Thus, PCR analysis demonstrated that the terminal duplications observed at fused chromosome ends were connected to the fused chromosome ends, which suggested that these duplications seal end-to-end fusions of critically shortened telomeres.

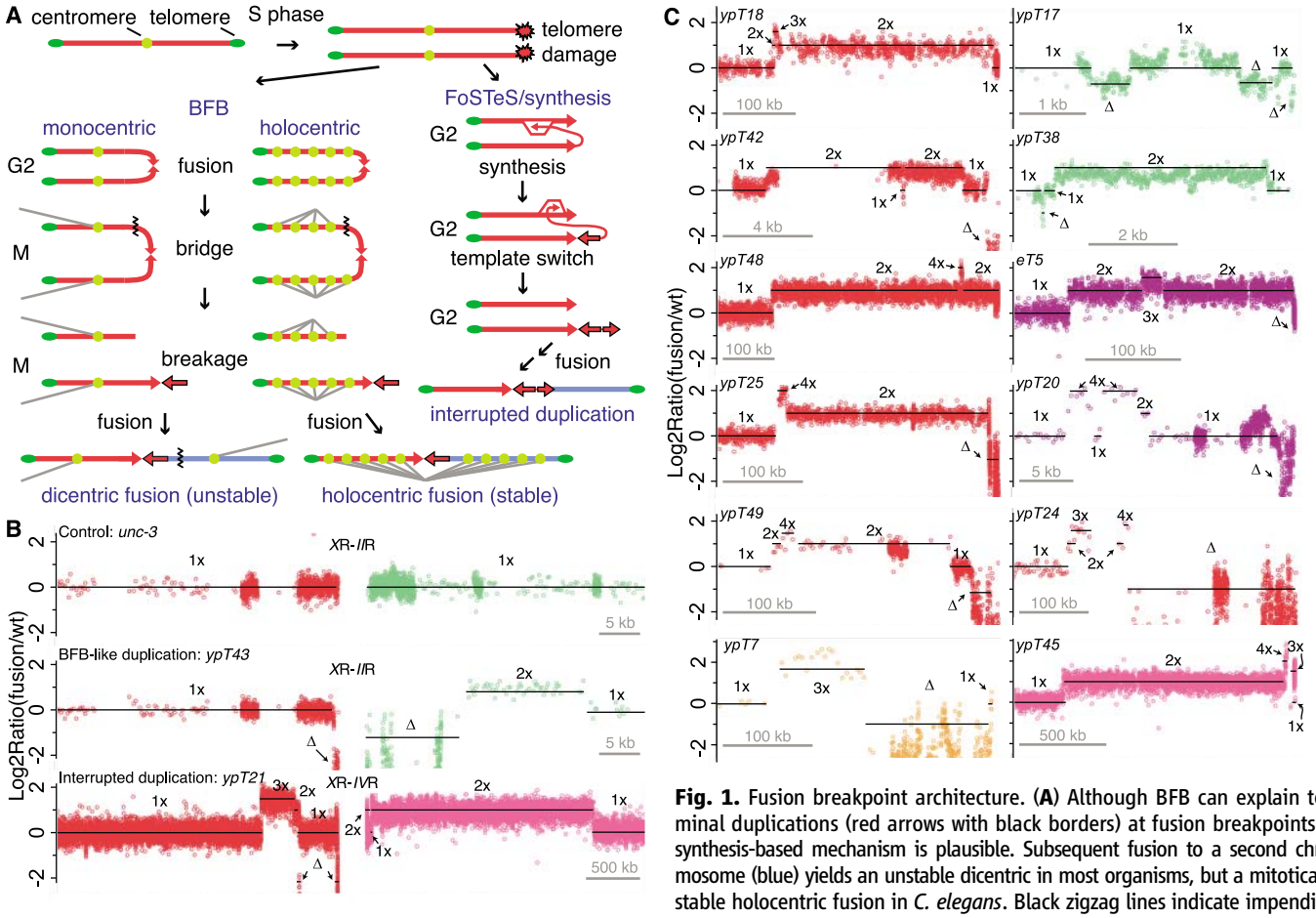

Fig. 1. Fusion breakpoint architecture. (**A**) Although BFB can explain terminal duplications (red arrows with black borders) at fusion breakpoints, a synthesis-based mechanism is plausible. Subsequent fusion to a second chromosome (blue) yields an unstable dicentric in most organisms, but a mitotically stable holocentric fusion in *C. elegans*. Black zigzag lines indicate impending breaks. (**B**) CGH plots of an *unc-3* control with normal chromosome termini and of fusion strains with duplications at fused chromosome termini. Telomeres are in center. (**C**) Chromosome ends bearing interrupted duplications. Telomeres are on the right side of CGH plots. The *y* axes represent the ratio of signal intensity for fusion versus wild type. The *x* axes represent the distance from a chromosome end, where green, purple, pink, tan and red indicate chromosomes *II*, *III*, *IV*, *V*, and *X*, respectively. Symbols: Δ (terminal or internal deletion), 1× (wild-type copy number), 2× (duplication), 3× (triplication), 4× (quadruplication).

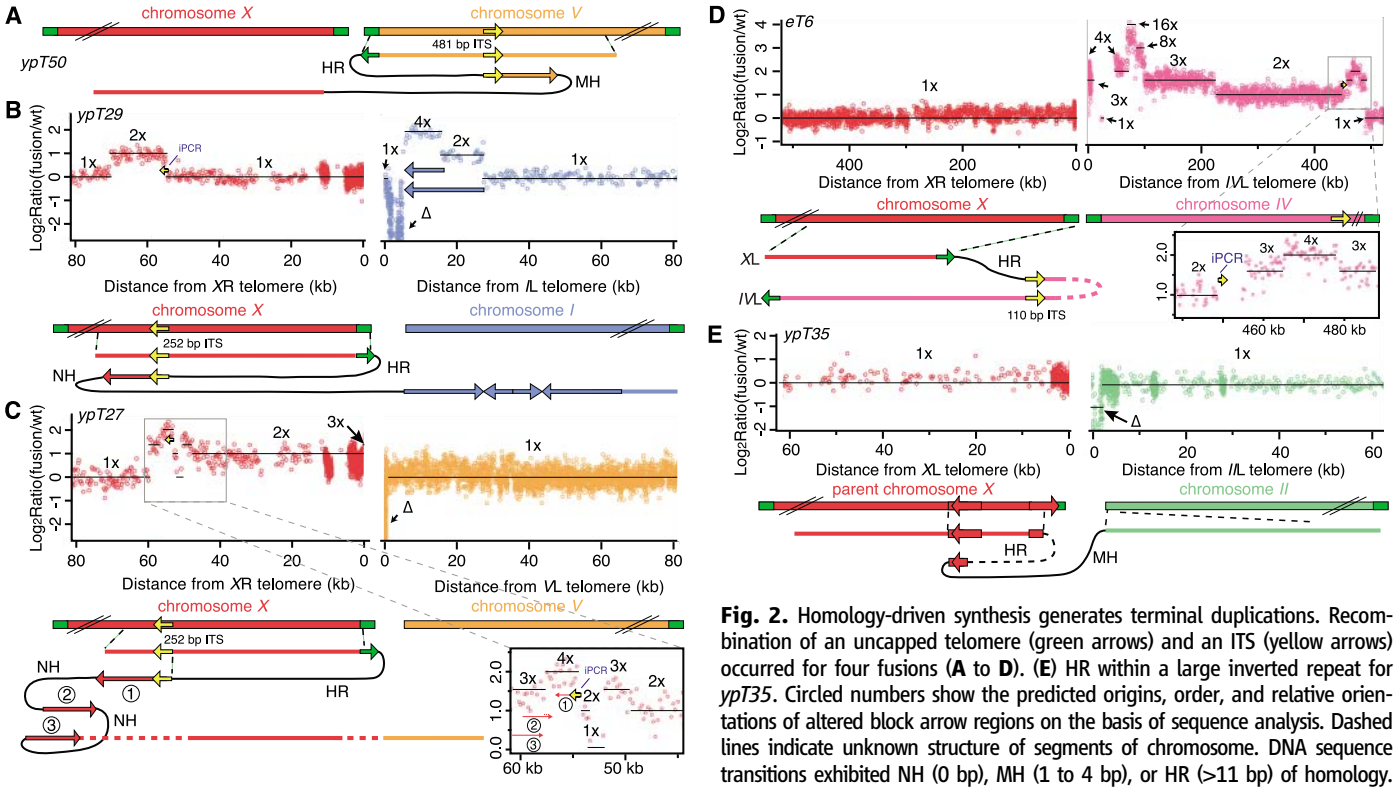

Fig. 2. Homology-driven synthesis generates terminal duplications. Recombination of an uncapped telomere (green arrows) and an ITS (yellow arrows) occurred for four fusions (**A** to **D**). (**E**) HR within a large inverted repeat for *ypT35*. Circled numbers show the predicted origins, order, and relative orientations of altered block arrow regions on the basis of sequence analysis. Dashed lines indicate unknown structure of segments of chromosome. DNA sequence transitions exhibited NH (0 bp), MH (1 to 4 bp), or HR (>11 bp) of homology. Plots follow same scheme as Fig. 1.

Most rearrangement junctions shared either no homology (NH) or one to four nucleotides of microhomology (MH), which suggested that they might have been products of nonhomologous end-joining (NHEJ) events (table S4). However, several fusion breakpoints contained longer stretches of homology (HR) corresponding to the telomeric repeat sequence TTAGGC. In the genome of *C. elegans*, many interstitial telomere sequence tracts (ITS) appear within the terminal 5 Mb of each chromosome end; they range in size from 12 bp to 486 bp and consist of perfect telomere repeats interspersed among degenerate telomere repeats (fig. S6). During creation of three fusions—*ypT50*, *ypT29*, and *ypT27*—an uncapped telomere recombined with the ITS located closest to its chromosome terminus, presumably the ITS of a sister chromatid (Fig. 2, A to C, and figs. S7 and S8). For *eT6*, an interchromosomal telomere recombination event occurred where the *X*L telomere recombined with the fifth ITS from the *IV*L terminus (Fig. 2D and fig. S6). These four fusion breakpoints could have been formed if strand transfer occurred within or adjacent to the longest stretch of perfect telomere repeat sequence in each ITS. The identical 25-nucleotide sequence within the terminal *X*R ITS was targeted for *ypT27* and *ypT29* (fig. S6). The amount of perfect telomere sequence remaining at the telomere recombination sites of *ypT29*, *ypT27*, *ypT50*, and *eT6* was 29.5, 16.7, 18, and 24.7 repeats, respectively. Telomeres can adopt a highly conserved strand invasion structure termed the T loop, whose minimal size in vitro is 148 bp or 24.7 repeats (*11*). Thus, telomere uncapping in the context of telomerase deficiency may result from an inability to form T loops that may protect chromosome termini from aberrant recombination events (*12*, *13*).

Although telomere recombination events have been observed for genomic DNA containing end-to-end fusions from human cells and from *C. elegans* (*14*, *15*), their consequences have not been reported previously. The *ypT27* and *eT6* telomere recombination events each resulted in interrupted duplications (Fig. 2, C and D). Recombination occurred at ITS tracts facing away from a chromosome end, yet elicited copy number changes on both sides of the targeted ITS, including much of the sequence between the ITS and its chromosome terminus (Fig. 2, C and D). The *ypT27* and *eT6* structures are inconsistent with BFB cycles or break-induced replication (BIR), where a new replication fork is established at a site of homology at least 72 bp in length, followed by precise duplication of the chromosome terminus (*16*, *17*). Instead, multiple template switching and synthesis initiation events may create duplications at uncapped telomeres (fig. S8). The *ypT29* and *ypT50* telomere recombination events each resulted in uninterrupted inverted duplications of 16 or 8 kb, respectively, structures that appear consistent with BFB (Fig. 2, A and B, and fig. S7). However, the template-switching events observed for *ypT27* and *eT6* telomere recombination events suggest that the inverted duplications that sealed *ypT29* and *ypT50* may have been template-based and created by synthesis-dependent strand annealing (SDSA) (*18*), where a simple break-primed synthesis reaction occurs and is resolved by an NHEJ reaction with a second uncapped telomere.

Two additional complex fusions occurred at the left end of the *X* chromosome, which ends with a 5-kb terminal inverted repeat that is separated by ~10 kb of intervening sequence. For *ypT35* and *ypT37*, 0.8- and 1.9-kb tracts of DNA adjacent to the internal copy of a 5-kb inverted repeat were added to *X*L before end-joining with the left end of chromosome *II* (Fig. 2E and fig. S9). Thus, strand invasion of the terminal *X*L repeat with the internal copy may have initiated an SDSA-like process, resulting in inverted uninterrupted duplications analogous to those of *ypT29* and *ypT50* (Fig. 2, A and B). Similar SDSA-like events may serve to initiate synthesis-mediated interrupted duplications (Fig. 1, B and C, and Fig. 2, C and D). Seven additional fusions exhibit breakpoints at either 23 or 300 kb from the *X*L telomere, which suggested recurrent locus-driven repair events (figs. S10 to 12).

Up to 32% of tumor genome fusion breakpoints show evidence of template switching, where segments of DNA near the breakpoint are duplicated and accompanied by deletion of intervening sequences (*19*–*21*). Such break-

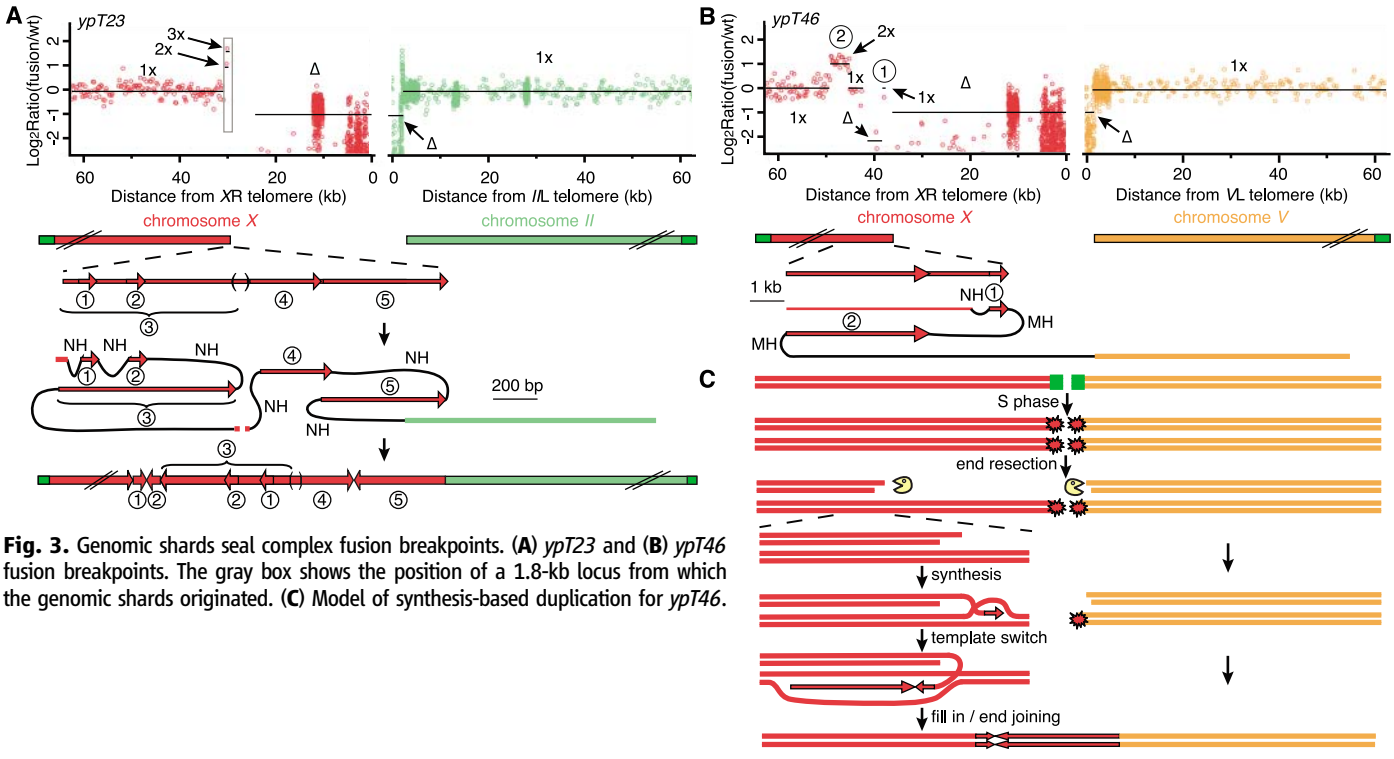

Fig. 3. Genomic shards seal complex fusion breakpoints. (**A**) *ypT23* and (**B**) *ypT46* fusion breakpoints. The gray box shows the position of a 1.8-kb locus from which the genomic shards originated. (**C**) Model of synthesis-based duplication for *ypT46*.

points are referred to as genomic shards or junctional sequences (*19*, *21*). This molecular signature was apparent from sequence analysis for one telomeric recombination event that was initiated by template-switching events, *ypT27* (Fig. 2C and fig. S8), and for three additional fusion events, *ypT23*, *ypT46*, and *ypT49* (Fig. 3 and fig. S13).

Large-scale duplication of interstitial segments of the human genome can result in genomic disorders. These aberrations display hallmarks that we observed in 82% of end-to-end fusions ($n = 38$): duplications interrupted by triplications and nonduplicated sequences, likely generated by template-switching, as well as breakpoints that are sealed by microhomology (*22*), which suggested a conserved process that may be relevant to metazoan genome evolution. Models where a stalled replication fork or double-strand break induces promiscuous DNA synthesis—termed fork stalling and template switching (FoSTeS) or microhomology-mediated BIR (mmBIR)—have been proposed to explain the origin of such large spontaneous mitotic duplications (Fig. 2, C and D, 3 and fig. S13) (*23*, *24*). Transposon excision in *C. elegans* can lead to duplications that may result from template switching (*25*), consistent with a role for replication-based repair in nonterminal segments of nematode genomes.

Although DNA bridges during mitosis are observed in cells with critically shortened telomeres, even in *C. elegans* (*5*), we propose that critically shortened telomeres commonly trigger synthesis events primed by microhomology or limited homology to create large-scale, interrupted subtelomeric duplications, in the absence of BFB cycles (Figs. 1; 2, C and D; and 3; and figs. S8 and S13). These interrupted duplications resemble interstitial mammalian genome aberrations attributed to FoSTeS or mmBIR, and they can be resolved by end-joining with a second dysfunctional chromosome end. BFB may function independently to promote duplication at uncapped telomeres before fusion.

Studies in *E. coli* have shown that genome duplications can occur in response to stress through a process similar to FoSTeS, and this has been hypothesized to be adaptive during evolution (*19*, *26*, *27*). Telomere dysfunction drives amplification and deletion of genomic loci relevant to human cancer (*28*). Recurrent or nonrecurrent recombination events similar to those described here could contribute to genome rearrangements that play critical roles in tumor development (*2*).

References and Notes

1. R. Capper *et al.*, *Genes Dev.* **21**, 2495 (2007).
2. S. M. Bailey, J. P. Murnane, *Nucleic Acids Res.* **34**, 2408 (2006).
3. B. McClintock, *Genetics* **26**, 234 (1941).
4. S. Ahmed, J. Hodgkin, *Nature* **403**, 159 (2000).
5. B. Meier *et al.*, *PLoS Genet.* **2**, e18 (2006).
6. Materials and methods are available as supporting material on *Science* Online.
7. M. R. Lowden, B. Meier, T. W. Lee, J. Hall, S. Ahmed, *Genetics* **180**, 741 (2008).
8. A. Kallioniemi *et al.*, *Science* **258**, 818 (1992).
9. K. K. Mantripragada *et al.*, *Int. J. Mol. Med.* **13**, 273 (2004).
10. N. Shimizu, K. Shingaki, Y. Kaneko-Sasaguri, T. Hashizume, T. Kanda, *Exp. Cell Res.* **302**, 233 (2005).
11. R. M. Stansel, T. de Lange, J. D. Griffith, *EMBO J.* **20**, 5532 (2001).
12. M. Raices *et al.*, *Cell* **132**, 745 (2008).
13. J. D. Griffith *et al.*, *Cell* **97**, 503 (1999).
14. I. Cheung, M. Schertzer, A. Rose, P. M. Lansdorp, *Nucleic Acids Res.* **34**, 96 (2006).
15. B. T. Letsolo, J. Rowson, D. M. Baird, *Nucleic Acids Res.* **38**, 1841 (2010).
16. G. Bosco, J. E. Haber, *Genetics* **150**, 1037 (1998).
17. J. A. Hackett, D. M. Feldser, C. W. Greider, *Cell* **106**, 275 (2001).
18. M. McVey, D. Radut, J. J. Sekelsky, *Genetics* **168**, 2067 (2004).
19. G. R. Bignell *et al.*, *Genome Res.* **17**, 1296 (2007).
20. P. J. Campbell *et al.*, *Nat. Genet.* **40**, 722 (2008).
21. P. J. Stephens *et al.*, *Nature* **462**, 1005 (2009).
22. J. A. Lee, C. M. Carvalho, J. R. Lupski, *Cell* **131**, 1235 (2007).
23. P. J. Hastings, J. R. Lupski, S. M. Rosenberg, G. Ira, *Nat. Rev. Genet.* **10**, 551 (2009).
24. D. Branzei, M. Foiani, *Cell* **131**, 1228 (2007).
25. D. G. Moerman, J. E. Kiff, R. H. Waterston, *Nucleic Acids Res.* **19**, 5669 (1991).
26. P. Stankiewicz, J. R. Lupski, *Annu. Rev. Med.* **61**, 437 (2010).
27. A. Slack, P. C. Thornton, D. B. Magner, S. M. Rosenberg, P. J. Hastings, *PLoS Genet.* **2**, e48 (2006).
28. R. C. O'Hagan *et al.*, *Cancer Cell* **2**, 149 (2002).

29. We thank J. Maydan for technical assistance; D. Reiner, J. Sekelsky, L. Shtessel, D. Shippen, and T. Petes for comments on the manuscript; and D. Ramsden for discussion. S.A. and M.L. were supported by NIH grants GM066228 and GM072150. D.G.M. was supported by funds from Genome Canada and Genome British Columbia and the Michael Smith Research Foundation. D.G.M. is a fellow of the Canadian Institute for Advanced Research.

Supporting Online Material

www.sciencemag.org/cgi/content/full/332/6028/468/DC1
Materials and Methods
SOM Text
Figs. S1 to S13
Tables S1 to S6
References

13 October 2010; accepted 18 March 2011
10.1126/science.1199022